

Ultrasonic relaxation from trapped hydrogen in rapidly cooled niobium

K. F. Huang and A. V. Granato

Department of Physics and Materials Research Laboratory, University of Illinois at Urbana-Champaign, Urbana, Illinois 61801

H. K. Birnbaum

Department of Metallurgy and Materials Research Laboratory, University of Illinois at Urbana-Champaign, Urbana, Illinois 61801

(Received 26 December 1984)

A relaxation in the ultrasonic response of rapidly cooled niobium containing hydrogen and oxygen is found. Measurements of attenuation and velocity as a function of temperature, frequency, polarization, hydrogen isotope, and annealing temperature are made. Evidence is obtained that the quenched-in defect is an OH_2 complex with tetragonal symmetry.

I. INTRODUCTION

Ultrasonic measurements on Nb-O-H alloys by Poker, Setser, Granato, and Birnbaum¹ showed an attenuation peak near 2.4 K at 10 MHz with a large isotope effect. The defect responsible for the peak was identified as hydrogen trapped at an oxygen interstitial. Similar relaxation phenomena have been reported by several other investigators.²⁻⁴

Quenching experiments on Nb with dilute concentrations of O and H by Hanada⁵ showed a resistivity increase at low temperatures, which was interpreted as indicating that hydrogen interstitials were frozen into the lattice by the quench. Most of the quenched-in resistivity annealed out between 4.2 and 100 K with two major recovery stages, one centered at 40 K and the other at 80 K. The 80-K stage was observed only in specimens with high oxygen content. The data were interpreted in terms of detrapping of hydrogen from oxygen interstitials. However, since Pfeiffer and Wipf⁶ had shown that the O-H pair was rather stable at 80 K, it was suggested by Hanada that the quenched-in defects were OH_n complexes with $n \sim 2-4$.

In the present work, measurements of ultrasonic attenuation and velocity in dilute Nb-O-H alloys were made as a function of temperature, frequency, polarization, concentration, annealing temperature, and hydrogen isotope. In addition to the stable relaxation peak near 2 K (peak 1) observed by Poker *et al.*,¹ an additional low-temperature peak (peak 2) was found when the specimens were rapidly cooled to helium temperature. In this paper, the characteristics of this new relaxation effect are described and the defect responsible is identified.⁷

II. EXPERIMENTAL PROCEDURE

Measurements were carried out on large single crystals of Nb purified by UHV annealing (2500 K at about 10^{-9} Pa) and having flat and parallel {100} and {110} faces. These faces were prepared using standard techniques and allowed acoustic measurements to be made to frequencies above 70 MHz. The major impurities in these specimens were as follows: Ta, ~ 100 at. ppm; C, 65 at. ppm; and N,

65 at. ppm. The O interstitial trap concentration was varied by controlling the O_2 partial pressure during the UHV annealing after the initial purification. Hydrogen or deuterium charging was carried out from the gas phase using gases purified by diffusion through a Pd-Ag membrane and the amount of H (D) charged was determined from the pressure-temperature-concentration (*P-T-C*) data and by weighing the crystals after charging.

Ultrasonic attenuation and velocity measurements were carried out using quartz transducers and standard techniques.⁸ A frequency change of 1 Hz, corresponding to a sensitivity of 2×10^{-7} in the elastic moduli, could be measured. The acoustic measurements were carried out in a cryostat which allowed rapid cooling of the specimens from 250 to 4 K at an average rate of about 2 K/s.

III. EXPERIMENTAL RESULTS

A. Hydrogen

Figure 1 shows a plot of decrement versus temperature for a 10-MHz *C'* mode in a niobium crystal containing about 100 ppm O and 700 ppm H after a "quench" from 240 to 4 K, followed by annealing at 70, 80, 90, 100, and 120 K. The decrement consists of a temperature-independent background due to bonding and diffraction losses, an electronic contribution proportional to the electrical conductivity, which decreases below the superconducting transition temperature, and two peaks due to hydrogen. The peak at 6.3 K anneals out near 80 K, while the peak at 2.4 K increases only a small amount. Both peaks were observed in the *C'* mode, but not in the *C*₄₄ mode suggesting that the defect responsible for peak 2 has a tetragonal symmetry.

Figure 2 shows the decrement versus temperature for three niobium specimens with differing oxygen contents after rapid cooling from 240 K. The hydrogen concentration is much greater than the oxygen concentration in each case. The background decrement has been subtracted in this figure. The peak heights scale with the oxygen concentration, while the electronic contribution decreases with increasing impurity content. The background attenuation at the Nb superconducting critical temperature

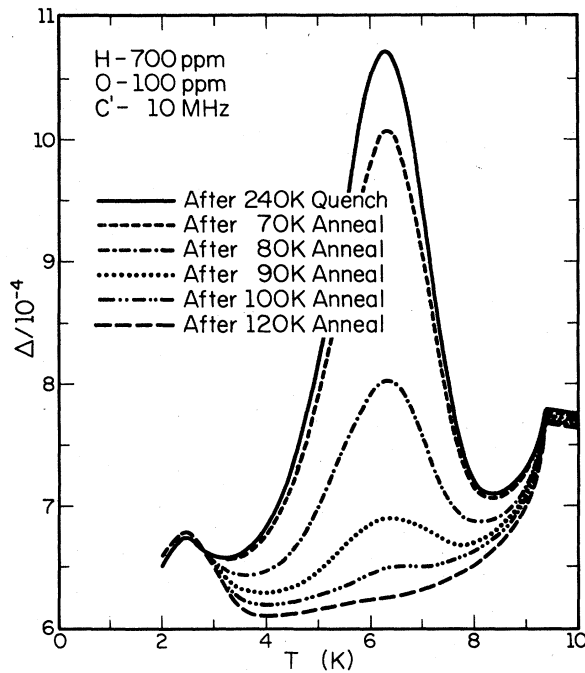


FIG. 1. Decrement versus temperature for a 10-MHz C' mode in a niobium crystal containing about 100 ppm O and 700 ppm H after a rapid cooldown from 240 K, followed by annealing at 70, 80, 90, 100, and 120 K. The rapid change of attenuation near 9.2 K is due to the transition from the normal to the superconducting state.

shows a decrease below T_c that is sensitive to the oxygen concentration. In the purest sample, the sharp decrease below T_c was large but peak 2 was small. However, in the sample with about 200 ppm oxygen, the decrease below T_c was hardly observed and peak 2 was large. After outgassing the hydrogen from the specimen, only a change in attenuation near T_c was found for each speci-

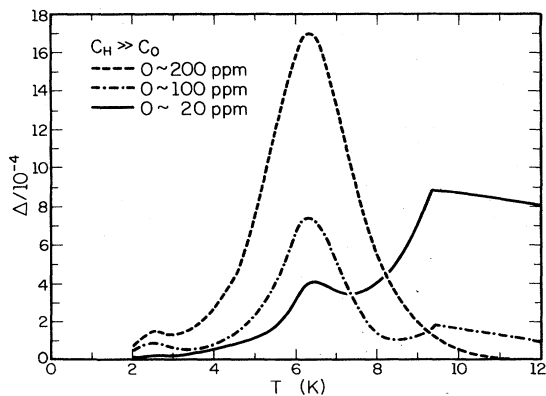


FIG. 2. Decrement versus temperature for three niobium specimens with differing oxygen concentrations after rapid cooling from 240 K. The magnitude of the attenuation change associated with the superconducting transition near 9.2 K is sensitive to the oxygen content. The heights of peak 1 and peak 2 are also related to the oxygen content.

men. The superconducting effect in the background attenuation near T_c serves as a monitor for the impurity content.

The decrement as a function of temperature for various frequencies, from 10 to 70 MHz, is shown in Fig. 3. The magnitude of the attenuation decrease below T_c increases as a function of increasing frequency. The shear-wave attenuation due to conduction electrons is given⁹ in the low-frequency limit (electron mean free path \ll ultrasonic wavelength) by

$$A = \left[\frac{2\pi^2 f^2}{\rho v^3} \right] (3\pi^2 N)^{2/3} \left[\frac{h^2 \sigma}{5e^2} \right], \quad (1)$$

where f is the frequency of the sound wave, ρ is the sample density, v is the sound velocity, N is the number of electrons of charge e per unit volume, and σ is the electrical conductivity (all in Gaussian units). The decrement can be obtained by $\Delta = A(\text{dB}/\mu \text{sec})/8.68f$ (MHz). Hence, the decrement scales linearly with frequency and conductivity. The resistivity⁵ due to oxygen in Nb is $5 \mu\Omega \text{ cm/at. \%}$; 100 ppm oxygen corresponds to $5 \times 10^{-2} \mu\Omega \text{ cm}$. The calculated decrement for 10 MHz is about 0.9×10^{-4} , which is smaller than the measured value 1.6×10^{-4} . Figure 3 also shows that the change of decrement below T_c scales about linearly with frequency.

The two peaks shift to higher temperatures as a function of increasing frequency. The relaxation time of peak 1 has been shown by Poker *et al.*,¹ to have an exponential temperature dependence with an activation energy of 1.8 meV. The relaxation time of peak 2 as a function of temperature is plotted in Fig. 4. The data can be fit with an apparent activation energy of 5.5 meV, and frequency factor of $3 \times 10^{11} \text{ s}^{-1}$.

The temperature dependence of the relaxation strength of peak 2 was obtained by plotting the peak heights (with the electronic contribution subtracted) as a function of inverse temperature, and is shown in Fig. 5. The uncertain-

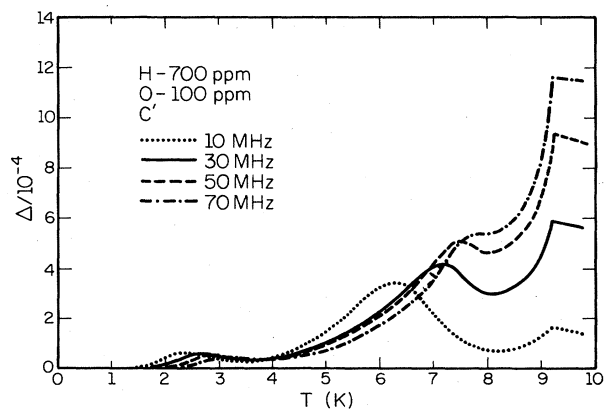


FIG. 3. Decrement as a function of temperature for various frequencies. The position of both peak 1 and peak 2 shift to higher temperatures as a function of increasing frequency. The attenuation change associated with the superconducting transition near 9.2 K is proportional to the frequency.

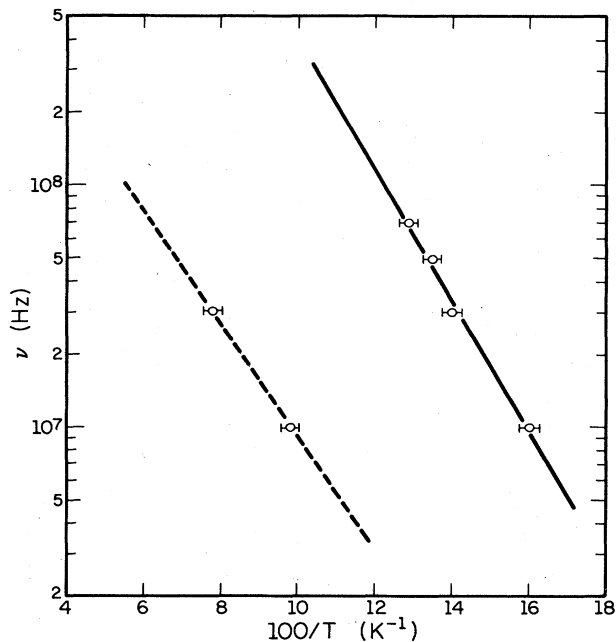


FIG. 4. Logarithm of relaxation frequency as a function of inverse temperature. The solid curve is a fit to the data points for the specimen quenched with hydrogen, while the two points connected with a dashed line are for deuterium.

ty in the relaxation strengths is due to the large superconducting effects at higher frequencies. The relaxation strength has a $1/T$ temperature dependence as expected for a classical relaxation, and does not show the quantum depletion effect observed for peak 1.

B. Deuterium

Figure 6 shows a plot of decrement versus temperature for a 10-MHz C' mode in a niobium crystal containing 100 ppm oxygen and 2000 ppm deuterium. Peak 1 and the sharp decrease of decrement below T_c are not evident due to the magnitude of peak 2, which appeared near 10.5 K with a high-temperature shoulder. Results for a 30-MHz C' mode are shown in Fig. 7. Extensive measurements were made only at 10 and 30 MHz due to the large

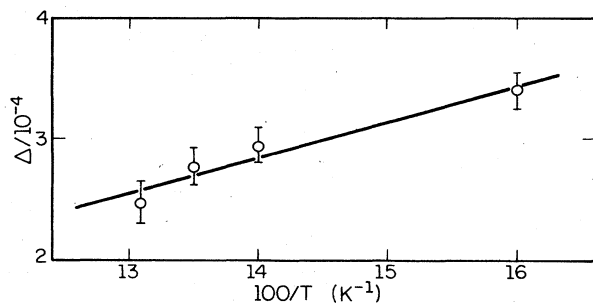


FIG. 5. Relaxation strength of peak 2 as a function of inverse temperature. The solid line is a $1/T$ fit.

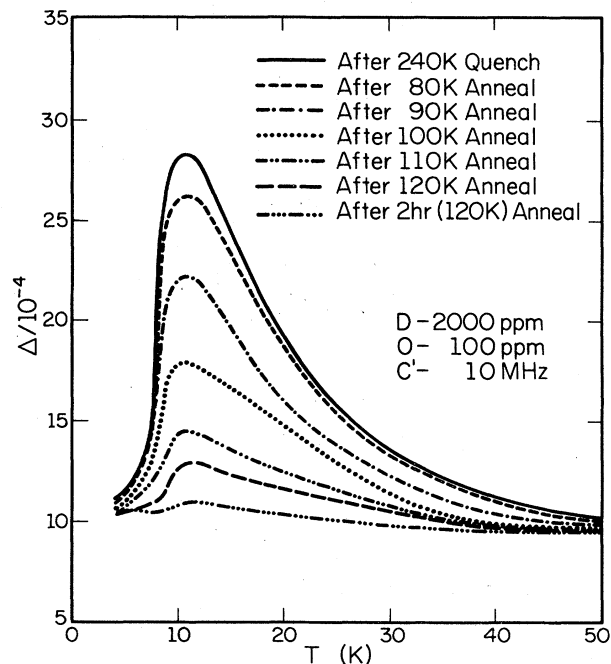


FIG. 6. Decrement versus temperature for a 10-MHz C' mode in a niobium crystal containing about 100 ppm O and 2000 ppm D after a rapid cooldown from 240 K, followed by annealing at 80, 90, 100, 110, and 120 K. Peak 2 appears at 10.5 K and has a high-temperature tail.

attenuation at higher frequencies. With data from only two relaxation frequencies, the temperature dependence of the relaxation time cannot be unambiguously determined. However, the peak shifts to higher temperatures as a

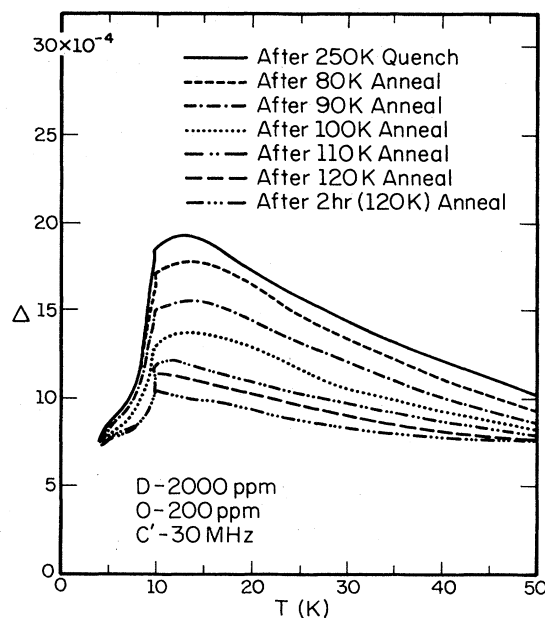


FIG. 7. Decrement versus temperature for a 30-MHz C' mode in a niobium crystal containing about 200 ppm O and 2000 ppm D after a rapid cooldown from 250 K, followed by annealing at 80, 90, 100, 110, and 120 K.

function of increasing frequency (Fig. 4) and if an Arrhenius dependence is assumed, the apparent activation energy and frequency factors are 4.6 meV and $1.8 \times 10^{11} \text{ s}^{-1}$, respectively.

C. Annealing behavior

As shown in Figs. 1, 6, and 7, annealing after the quench decreased the relaxation strength of peak 2 and resulted in a small increase in the height of peak 1. A detailed analysis of the annealing behavior required deconvolution of the two peaks, which was difficult due to the disparity of heights and their overlap. This deconvolution was carried out for each annealing temperature assuming that each peak has a shape which does not change during annealing.

Figure 8 shows the normalized magnitude of each peak after a 10-min anneal at the indicated temperature. Peak 1 increases by about 15% while peak 2 anneals out. The linear relation between the peak heights of peak 1 (h) versus those of peak 2 (H) at each annealing temperature indicates that the defects causing peak 2 convert to the defects causing peak 1 during annealing (see Fig. 9). Since peak 2 is about 6 times larger than peak 1 and the defect concentration of peak 2 is only about 15% that of peak 1, the relaxation strength of peak 2 may be estimated to be about $6/0.15 = 40$ times greater than that of peak 1.

D. Velocity measurements

Acoustic velocity measurements were made from 0.6 to 20 K after slow cooling and quenching from 240 K on a sample with 100 ppm oxygen and 700 ppm hydrogen. The frequency change as a function of temperature is

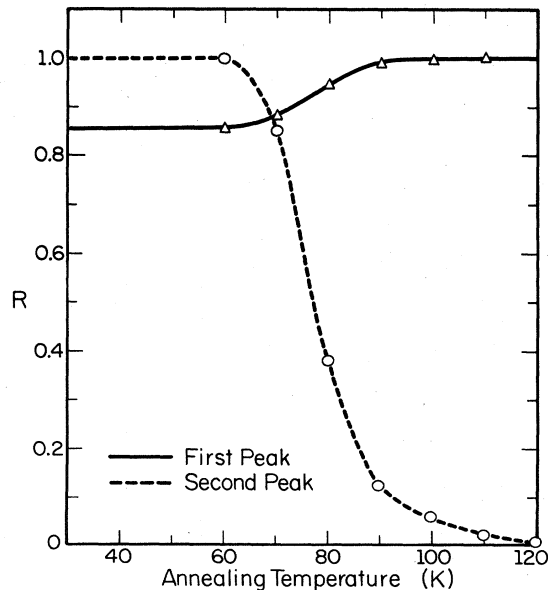


FIG. 8. Annealing behavior of the two peaks. The solid and dashed curves represent the normalized magnitude of each peak after a 10 min anneal at the indicated temperature. Peak 1 increases by about 15% while peak 2 anneals out.

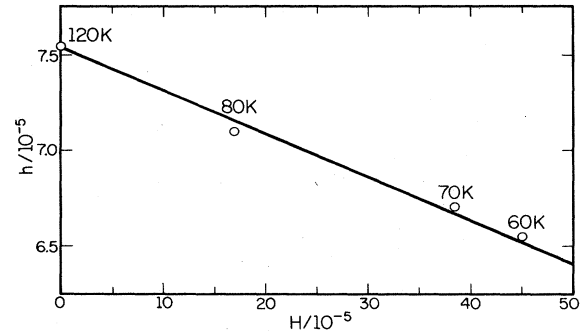


FIG. 9. Height of peak 1 (h) versus that of peak 2 (H) at annealing temperatures 60, 70, 80, and 120 K.

plotted in Fig. 10. The magnitude of the decrease below 2 K is larger than that observed by Poker *et al.*¹ due to the fact that this sample had only 100 ppm oxygen and hence had less internal strain; the modulus defect below peak 1 is expected to decrease with internal strain. The dispersion at 2.5 K is apparently due to peak 1, which is present in both slow- and fast-cooling processes while the dispersion around 6 K is seen only in a fast-cooling process. The dispersion associated with peak 2 suggests that it is due to a relaxation process.

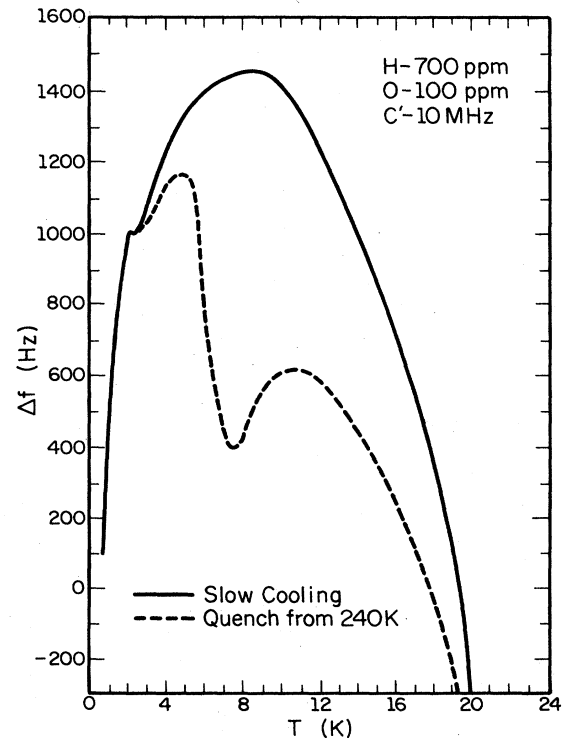
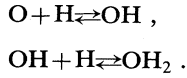


FIG. 10. Frequency change versus temperature for a 10-MHz C' mode in a niobium crystal containing about 100 ppm O and 700 ppm H. The solid curve represents the result of a slow-cooling process and the dashed curve represents that of a fast cooling from 240 K. The small dispersion near 2 K is seen after both slow- and fast-cooling processes. The dispersion near 6 K is present only in the fast-cooling process.

IV. DISCUSSION

Peak 2 annealed out at the same temperature, for specimens containing H and D, as did the resistivity annealing stages found by Hanada⁵ for quenched specimens; thus, suggesting that the same defect is responsible for the resistivity and anelastic behavior. The dependence of the data on oxygen concentration suggests that the defect responsible for peak 2 is associated with oxygen interstitials. Since these peaks are observed only in specimens containing H or D, the relevant defect is an O-H(D) complex. Peak 1 has been shown¹ to be caused by a single H (D) at an O. The correlation between peak 1 and peak 2 during annealing suggests that peak 2 arises from an OH₂ complex. In a slow-cooling process, one oxygen traps only one hydrogen at low temperatures, and this O-H pair is rather stable.⁶ In a rapid cooling process, some of the oxygen may trap more than one hydrogen, forming an OH₂. However, the second hydrogen is less strongly bound than the first one and during annealing, detrapping of one of the two hydrogens occurs, converting the OH₂ to an OH with the freed hydrogen adding to the precipitated hydride formed by the untrapped H.

This simple interpretation can be supported quantitatively using rate theory. In the temperature range of interest, hydrogen atoms are mobile in the lattice with a migration energy of E_m , and oxygen interstitials are immobile. Interactions of hydrogen with the O traps results in formation of OH and OH₂ as expressed by



The rate equations describing these reactions are

$$\begin{aligned} \frac{dC_{\text{OH}}}{dt} &= \nu C_{\text{O}} C_{\text{H}} \exp(-E_m/kT) \\ &\quad - \nu C_{\text{OH}} \exp[-(E_1 + E_m)/kT] \\ &\quad + \nu C_{\text{OH}_2} \exp[-(E_2 + E_m)/kT] \\ &\quad - \nu C_{\text{H}} C_{\text{OH}} \exp(-E_m/kT), \end{aligned} \quad (2)$$

$$\begin{aligned} \frac{dC_{\text{OH}_2}}{dt} &= -\nu C_{\text{OH}_2} \exp[-(E_2 + E_m)/kT] \\ &\quad + \nu C_{\text{H}} C_{\text{OH}} \exp(-E_m/kT), \end{aligned} \quad (3)$$

where C_{H} , C_{O} , C_{OH} , C_{OH_2} are the hydrogen, oxygen, OH, and OH₂ concentrations, respectively, E_m is the migration energy of hydrogen, E_1 is the binding energy between O and H, E_2 is the binding energy between OH and H, and ν is the vibrational frequency which, as a simplify-

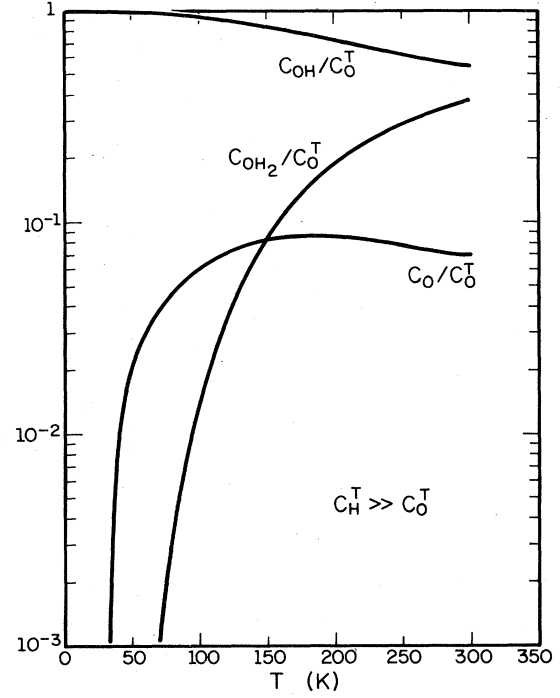


FIG. 11. Calculated equilibrium concentrations of $C_{\text{OH}}/C_{\text{O}}^T$, $C_{\text{OH}_2}/C_{\text{O}}^T$, and $C_{\text{O}}/C_{\text{O}}^T$ versus temperature.

ing approximation, is taken to be the same for hydrogen in any configuration (H, OH, or OH₂). Conservation of total H and O further requires

$$C_{\text{H}}^T = C_{\text{H}} + C_{\text{OH}} + 2C_{\text{OH}_2}, \quad (4)$$

$$C_{\text{O}}^T = C_{\text{OH}} + C_{\text{OH}_2} + C_{\text{O}}, \quad (5)$$

where C_{H}^T and C_{O}^T are the total hydrogen and oxygen concentrations exclusive of any precipitated hydride.

Since $C_{\text{H}}^T \gg C_{\text{O}}^T$ in all the experiments, the hydrogen concentration is determined by equilibrium with the β hydride which results in

$$C_{\text{H}} = a \exp(-\Delta\mathcal{H}/kT). \quad (6)$$

$\Delta\mathcal{H}$ and a have been determined⁶ to be 0.12 ± 0.015 eV and 4.7 ± 0.9 , with C_{H} as the ratio of the hydrogen concentration to the niobium concentration $[\text{H}]/[\text{Nb}]$.

In thermal equilibrium one has $dC_{\text{OH}}/dt = 0$ and $dC_{\text{OH}_2}/dt = 0$, whence

$$C_{\text{OH}_2} = C_{\text{H}} C_{\text{OH}} \exp(E_2/kT), \quad (7)$$

$$C_{\text{OH}} = C_{\text{H}} C_{\text{O}} \exp(E_1/kT). \quad (8)$$

Then, one can solve Eqs. (5)–(8) for C_{OH_2} and C_{OH} . The solutions are

$$\frac{C_{\text{OH}_2}}{C_{\text{O}}^T} = \frac{a^2 \exp[(E_1 + E_2 - 2\Delta\mathcal{H})/kT]}{a^2 \exp[(E_1 + E_2 - 2\Delta\mathcal{H})/kT] + a \exp[(E_1 - \Delta\mathcal{H})/kT] + 1}, \quad (9)$$

$$\frac{C_{\text{OH}}}{C_{\text{O}}^T} = \frac{a \exp[(E_1 - \Delta\mathcal{H})/kT]}{a^2 \exp[(E_1 + E_2 - 2\Delta\mathcal{H})/kT] + a \exp[(E_1 - \Delta\mathcal{H})/kT] + 1}. \quad (10)$$

These equilibrium concentrations depend sensitively on the values of E_1 , E_2 , and $\Delta\mathcal{H}$ and these are not all known. Values for $\Delta\mathcal{H}$ and E_1 may be obtained from the resistivity measurements of Pfeiffer and Wipf.⁶ The binding energy of the second H to the O, E_2 , must be less than E_1 , since after slow cooling C_{OH} (associated with peak 1) is larger than C_{OH_2} (associated with peak 2). No significant peak-2 amplitude is observed in slow-cooled specimens. The equilibrium values of C_{OH} and C_{OH_2} were calculated (Fig. 11) for $E_1=0.13$ eV, $E_2=0.07$ eV, $\Delta\mathcal{H}=0.12$ eV, $a=4.7$, $C_O^T=100$ ppm, and $C_H^T > C_O^T$.

At 300 K, $C_{OH}/C_O^T \approx 0.55$, and $C_{OH_2}/C_O^T \approx 0.4$. As the temperature is decreased the OH_2 concentration decreases and the OH concentration increases. At 4 K, only OH complexes would be expected with the excess hydrogen forming β hydride in agreement with the observation that only peak 1 is observed after slow cooling. During a quench, however, a distribution characteristic of an elevated temperature will be frozen in and a significant C_{OH_2} will be retained. During subsequent annealing, the equilibrium concentrations will be attained and peak 2 should decrease as is observed. The rate-limiting step in this annealing is the dissociation of OH_2 , $OH_2 \rightarrow OH + H$, with an activation enthalpy of $(E_2 + E_m)$. Since E_m is about 0.1 eV the annealing out of peak 2 is characterized by a process having an enthalpy of about 0.17 eV and hence should occur in the 80-K temperature range observed. A concomitant increase in peak 1 is expected as the OH concentration increases. Since the annealing data

(Fig. 8) showed that the quenched-in configuration had a C_{OH_2}/C_{OH} ratio of 6, the "freeze-in" temperature may be estimated from Fig. 11 to be about 170 K.

V. SUMMARY

An ultrasonic relaxation has been observed in specimens of rapidly cooled niobium containing oxygen and hydrogen at 6.3 K at 10 MHz. This relaxation is closely related to the previously reported OH relaxation observed at about 2 K at 10 MHz. The rapidly changing ultrasonic attenuation background is strongly dependent on the O concentration and can be used to monitor the purity of the specimens. The 6.3-K relaxation corresponds to a defect having tetragonal symmetry and a strong isotope effect. The annealing behavior of the relaxation provides evidence that the relaxing defect is an OH_2 complex, formed at some of the oxygen interstitial trapping centers during rapid cooling. The second hydrogen is less strongly bound to the oxygen interstitial than the first. During the annealing, detrapping of one of the hydrogen occurs and the OH_2 converts to an OH defect with the freed hydrogen adding onto the β hydride precipitates.

ACKNOWLEDGMENT

This work was supported by the Department of Energy, Division of Materials Sciences under Contract No. DE-AC02-76ER01198.

¹D. B. Poker, G. G. Setser, A. V. Granato, and H. K. Birnbaum, *Z. Phys. Chem.* **260**, 636 (1979).

²G. Cannelli and R. Cantelli, *Solid State Commun.* **43**, 567 (1982).

³G. Cannelli, R. Cantelli, and G. Veretchi, *Appl. Phys. Lett.* **39**, 832 (1981).

⁴G. Bellessa, *J. Phys. Lett.* **44**, L387 (1983).

⁵R. Hanada, in *Proceedings of the Second International Congress on Hydrogen in Metals, Paris* (Pergamon, Oxford, 1977), Vol. 3, p. 1136.

⁶G. Pfeiffer and H. Wipf, *J. Phys. F* **6**, 167 (1976).

⁷A brief preliminary account of this was given in *Proceedings of the North Atlantic Treaty Organization International Symposium on the Electronic Structure and Properties of Hydrogen in Metals*, edited by P. Jena and C. B. Satterthwaite (Plenum, New York, 1983), p. 123.

⁸K. L. Hultman, Ph.D. thesis, University of Illinois at Urbana-Champaign, 1979.

⁹W. P. Mason, *Physical Acoustics and the Properties of Solids* (Van Nostrand, Princeton, New Jersey, 1958).